Efficient quantitative modelling of Herzberg-Teller vibronic twophoton absorption spectra of organic fluorophores: Enhancement of parity-forbidden transitions

Aleksander Trummal^a, Merle Uudsemaa^a, Charles W. Stark^a, Meelis-Mait Sildoja^a, Jüri Pahapill^a, Aleksander Rebane^{a,b}

^aNational Institute of Chemical Physics and Biophysics, Akadeemia tee 23, Tallinn, Estonia ^bMontana State University, 264 EPS, Bozeman, Montana, USA.

ABSTRACT

Two-photon absorption (2PA) transitions play a key role in numerous photonic applications, where many prominent features in the 2PA spectra of organic fluorophores are due to transitions between electronic-vibrational (vibronic) states. While quantum-chemical calculations excel at modelling purely electronic 2PA transitions, success in predicting vibronic properties remains limited. This is in part due to high computational costs of evaluating 2PA tensor derivatives required for Herzberg-Teller (HT) vibronic interactions, especially if carried out across full vibrational coordinate space of the chromophores. Here, we present a novel highly efficient and cost-effective approach to modelling of HT vibronic two-photon absorption spectra of organic fluorophores by using the latest version of FCclasses3 code combined with judicious pre-selection of symmetry-adapted vibrational subspace. We apply this method to a C_{2h} inversion-symmetric diketopyrrolopyrrole chromophore, where the 2PA spectrum is dominated by HT terms because Franck-Condon contributions vanish due to LaPorte rule. Our results are in excellent agreement with recently reported experimental 2PA spectra confirming two-photon HT coupling is indeed dominated by, B_u-symmetry modes, and is also consistent with the experimentally observed polarization ratio. However, nominally-forbidden features near the electronic-origin appear significantly larger than HT coupling permits, indicating the presence of additional phenomena.

Keywords: Two-photon absorption, HT coupling, FCHT 2PA vibronic model, 2PA tensor derivatives

1. INTRODUCTION

Two-photon absorption (2PA) spectra of organic fluorophores often include prominent vibronic features of crucial importance for diverse applications including the vast field of biological imaging and microscopy. For example, Rhodamine B, an organic dye used extensively for staining in fluorescence microscopy and other biotechnology applications, is characterized by enhanced 0-1 vibronic transition in the low-lying part of the 2PA spectrum. For the corresponding linear absorption, however, 0-0 electronic component clearly prevails while the frequency of normal mode shaping vibronic progression depends on spectroscopic modality. Such behavior is rather unexpected for noncentrosymmetric molecule where the shapes of one-photon and two-photon absorption profiles should be closely related to each other, based on assumed similarity in underlying Franck-Condon (FC) factors for these fully allowed electronic transitions. Similarly, in 2PA spectra of various fluorescent proteins (FP) being widely used as genetically encoded 2PA microscopy probes, the dominant feature in the low-energy spectral range is associated with the blue-shifted vibronic 0-1 transition.² This is again in stark contrast with respective linear absorption spectra where the strongest absorption is localized in the corresponding 0-0 region due to pure electronic transition. Understanding the nature of 2PA properties and ability to predict spectral intensity distribution in fluorescent proteins is essential for rational design of specific mutants with enhanced two-photon brightness in the desired spectral range. For chromophore moieties within protein structure where selection rules are relaxed because of the lack of formal inversion symmetry, one may expect that vibronic intensity distribution is mainly governed by FC factors. However, it has been shown previously that non-Condon effects are responsible for shaping 2PA profiles of a number of fluorescent proteins.²⁻⁴

Franck-Condon principle states that the intensity of the symmetry-allowed vibronic transition is proportional to the square of the overlap integral between the vibrational wavefunctions of the two involved states, assuming that electronic transition dipole moment (TDM) is unaffected by vibrational distortion during the transition. For symmetry-forbidden transitions

where $|\mu_{if}(Q_0'')| \simeq 0$, one needs to consider a variation of TDM during the transition, i.e. the second term in the Taylor series of TDM expansion about equilibrium geometry of one of the involved states, designated as Herzberg-Teller term:

$$\langle \Psi'_{fv} | \mu | \Psi''_{iv} \rangle = \mu_{if}(Q''_0) \underbrace{\langle \Psi'_{fv} | \Psi''_{iv} \rangle}_{\text{FC factor}} + \underbrace{\sum_{k=1}^{N} \left(\frac{\partial \mu_{if}}{\partial Q''_k} \right) \langle \Psi'_{fv} | Q''_k | \Psi''_{iv} \rangle}_{\text{HT term}} + \cdots$$
(1)

For the two-photon transition tensor S, being proportional to $\langle i|\mu_a|n\rangle\langle n|\bar{\mu}_b|f\rangle$, the analogous expansion is given by:

$$S_{i1i2}^{GK} = (S_{i1i2}^{GK})^0 + \sum_{j}^{N} \left(\frac{\partial S_{i1i2}^{GK}}{\partial Q_j} \right) Q_j + \cdots$$
 (2)

representing both zeroth-order FC and first-order HT terms.⁵

For cases like FP-s, while considering Taylor expansion of the two-photon transition tensor, both zeroth-order FC term as well as first-order HT term expressing variation of the two-photon transition tensor within vibrational coordinate space during the transition should be taken into account. Thereby, the HT approximation describes the effects of weak inter-state coupling for the well-separated states. Attempts to address prediction of non-Condon 2PA properties of FP-s have been scarce so far. These studies rely on either phenomenological model of 2PA cross-section expansion series in terms of the change in permanent electric dipole moment including both static (FC) and vibrationally-resolved (HT) contributions² or quantum chemical modeling employing approximated HT terms.³ So far, straightforward quantum-chemical prediction of non-Condon 2PA vibronic properties remains largely out of reach.^{4,6} This is in part due to high computational costs of evaluating 2PA tensor derivatives required for HT vibronic interactions, especially if carried out across full vibrational coordinate space of the chromophores, while required analytical framework and respective computational methods are still under development.⁷⁻¹¹ However, support for 2PA spectroscopy has been recently added in generally available FCclasses3 vibronic simulation package¹² which enables us to address calculation of vibrationally-resolved 2PA spectra by taking advantage of combined FC and HT expansion of 2PA tensor in fully consistent approach.

As a first step toward quantum chemical modeling of HT 2PA properties of fluorescent proteins as well as other chromophores where vibronic model may require expansion beyond the FC approximation, we use diketopyrrolopyrrole chromophore (PDP) as a model compound (Fig. 1) for testing a novel cost-effective approach for computing HT vibronic 2PA spectra relying on pre-selection of symmetry-adapted vibrational subspace.

Figure 1. Reversible switching of symmetry by protonation for the studied PDP (C_{2h}) and singly-protonated HPDP (C₁) chromophores.

The neutral form of a pH-sensitive inversion-symmetry switching PDP 13 conforms to the C_{2h} point group and has linear absorption S_0 - S_1 transition in the wavelength range, 400-550 nm (Fig. 2). The one-photon absorption (1PA) spectrum features a maximum at 508 nm, as well as a Franck-Condon vibronic progression featuring a second smaller peak at 475 nm. Owing to the formal B_u transition symmetry, LaPorte selection rules formally prohibit 2PA in the S_0 - S_1 for both purely electronic and FC transitions. However, this is in stark contrast to experimental observations, which show a maximum at 954 nm, and a shoulder near 1010 nm, closely matching the 1PA features at twice the wavelength. Because FC terms are electronically-forbidden, this hints at significant Herzberg-Teller vibrational coupling. Even though such situation is quite common in many different types of two-photon chromophores, high computational costs associated with evaluating numerical derivatives of the 2PA tensor over the entire vibrational space have so far imposed severe limitations on effective modeling. In contrast, the product of protonation equilibrium of PDP, designated as HPDP, lacks formal inversion symmetry and, therefore, LaPorte selection rules are relaxed for this protonation state. For singly-protonated HPDP, 1PA and 2PA profiles show remarkable similarity with the peaks at 546 nm and 1086 nm, respectively. Consequentially, in this case the 2PA vibronic progression of the allowed electronic transition is dominated by more easily accessible FC terms, closely resembling respective 1PA progression.

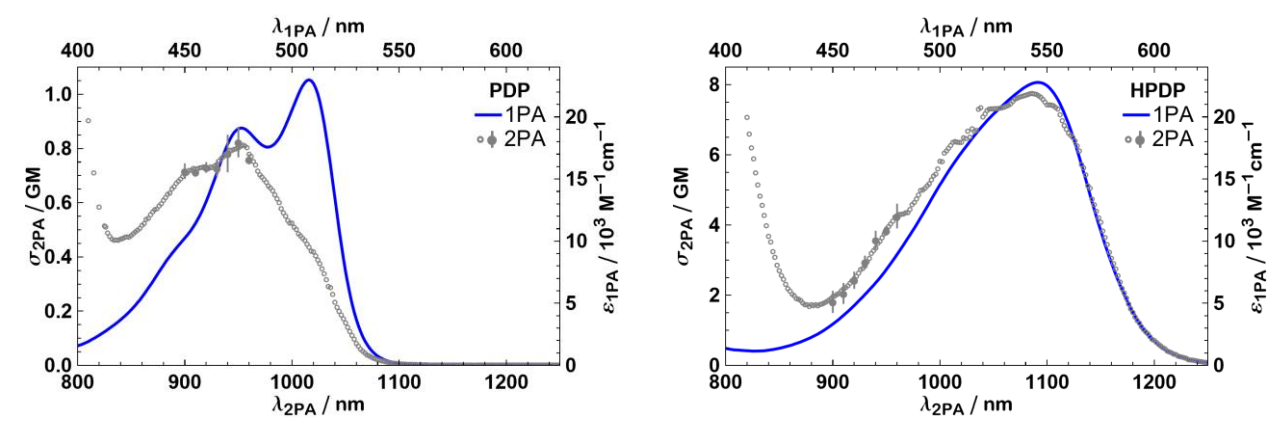


Figure 2. 1PA (blue line) and 2PA (gray dots) spectra of PDP and HPDP, respectively.

2. METHODS

Ground state conformational search for the PDP and HPDP chromophores was carried out both in the gas phase and in implicit methanol solvent at IEFPCM 14,15 /B3LYP 16,17 /6-311G(d,p) 18 level using the Gaussian16 19 software package and a lack of imaginary frequencies in harmonic vibrational analysis was observed for the optimized structures selected for subsequent TD-DFT 20 calculations of vertical electronic transitions. As C_{2h} point group constraints imposed on centrosymmetric structure of the PDP in methanol produced multiple imaginary eigenvalues associated with infinitesimal rotations of t-Bu end groups during vibrational normal mode analysis, the symmetry for this structure was lowered to C_2 while keeping closely matched orientations of t-Bu and maintaining correct energetic minima characteristics. Therefore, the quasi-centrosymmetric nature of this lowest-energy representative of the entire conformational space of PDP in methanol was preserved. The non-centrosymmetric HPDP structure in methanol is consistent with C_1 point group definition while respective C_s form of slightly higher energy is again associated with two vibrational modes with imaginary eigenvalues.

The CAM-B3LYP²¹ range-separated hybrid functional with mild Coulombic attenuation was tuned to achieve the best possible description of the first vertical singlet transition which is expected to be close to the energy of experimental absorption maxima. Consequently, the calculations of spectral properties for neutral PDP were carried out at IEF-PCM/mCAM-B3LYP ($\alpha=0.08$, $\beta=0.92$, $\mu=0.15$)/6-311G(d,p) level and the same definition was selected for respective calculations in the gas phase. The best match for protonated HPDP was observed at IEFPCM/mCAM-B3LYP ($\alpha=0.08$, $\beta=0.92$, $\mu=0.135$)/6-311G(d,p) level of theory. The variation of μ values within the range 0.135 – 0.150, along with selected combination of α and β values maintaining correct asymptotic behavior in the long-range limit, is consistent with our previous²² tuning of CAM-B3LYP functional for better description of charge transfer phenomena as compared to standard CAM-B3LYP. The use of slightly different μ values for neutral and charged species is justified due to varying extent of charge transfer in respective structures. These theoretical methods were used throughout the study for calculation of gradient and hessian values for both S₀ and S₁ states using Gaussian16 package, as well as for subsequent evaluation of respective 2PA transition tensors.

The quadratic response module of Dalton2018 software suite^{23,24} was used for 2PA calculations of PDP and HPDP in the gas phase and methanol. The corresponding second-order transition moment S_{ab}^{if} between the initial (i) and final (f) states is expressed as:

$$S_{ab}^{if}(\omega_1, \omega_2) = \sum_{n \neq i} \left\{ \frac{\langle i | \mu_a | n \rangle \langle n | \overline{\mu}_b | f \rangle}{\omega_{ni} - \omega_1} + \frac{\langle i | \mu_b | n \rangle \langle n | \overline{\mu}_a | f \rangle}{\omega_{ni} - \omega_2} \right\}$$
(3)

where $\langle i|\mu_a|n\rangle$ is the transition dipole moment between the corresponding electronic states along Cartesian axis a, ω_{ni} is the excitation energy, ω_1 and ω_2 are the frequencies of photons involved in transition (ω_1 and ω_2 are equal in case of 2PA). The derivatives of 2PA transition tensor along full set of ground-state vibrational eigenvectors of PDP were evaluated numerically by calculating the finite differences for positive and negative displacements applied to each normal mode. The subset of 2PA tensor derivatives along the normal modes of B_u symmetry was subsequently extracted from the full set.

The vibrationally-resolved $2PA^{25}$ spectra for $S_0 \rightarrow S_1$ transition in PDP were computed in the gas phase and in methanol using either time-independent $(TI)^{26-29}$ or time-dependent $(TD)^{30,31}$ vertical gradient $(VG)^{32}$ approach at T=0, 100, and 300 K as implemented in the FCclasses3 software¹², encompassing both FC and HT expansion terms. The selection of VG model is well justified because in case of forbidden electronic 2PA the signs of the derivatives of 2PA tensor are undefined. To achieve a good spectrum convergence for TI calculation, a maximum number of integrals evaluated for each excitation class was set to 10^6 . Likewise, the vibronic 2PA spectra of HPDP in methanol were calculated by using adiabatic hessian (AH) model, after the first excited state was optimized and corresponding frequency calculation have been carried out in implicit methanol solvent under equilibrium conditions. In this case, the S-tensor expansion included just FC terms as the 2PA transition is fully allowed for HPDP.

Two-photon polarization ratio measurements were performed using a previously described automated two-photon excited fluorescence spectrometer. Briefly, <170 fs pulses were generated using a 6 kHz laser and optical parametric amplifier pair (PHAROS-SP/ORPHEUS-HE, Light Conversion), continuously tunable over a signal range range of 630 - 1040 nm (with idler 1020 - 2600 nm) with a FWHM bandwidth of 7 - 16 nm. Polarization control was attained via a Glan-Laser polarizer and an achromatic $\lambda/4$ -waveplate (AQWP05M-980, Thorlabs), placed before the sample, and rotated to achieve vertical (V) or circular (R and L) excitation. Sample emission was collected at 90°, through a polarizer oriented at magic angle, 33 followed by a monochromator (Kymera 328i, Andor) and nitrogen cooled CCD (Symphony-Solo, Horiba). The polarization ratio (Ω) was obtained from four back-to-back spectral measurements R_1 - V_2 - L_3 - V_4 , calculated at each wavelength as, $\Omega = (R_1 + L_3)/(V_2 + V_4)$.

3. RESULTS

The main results showing the calculated 2PA vibronic spectra of PDP and HPDP are presented in Figures 3 and 4.

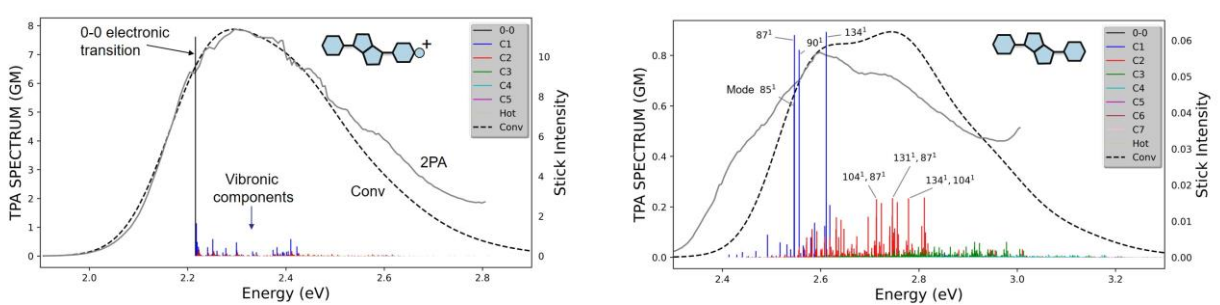


Figure 3. Calculated vibronic spectra of HPDP (TI, FC, Bu-subset), left panel and PDP (TI, FCHT, Bu-subset), right panel in MeOH at 300K.

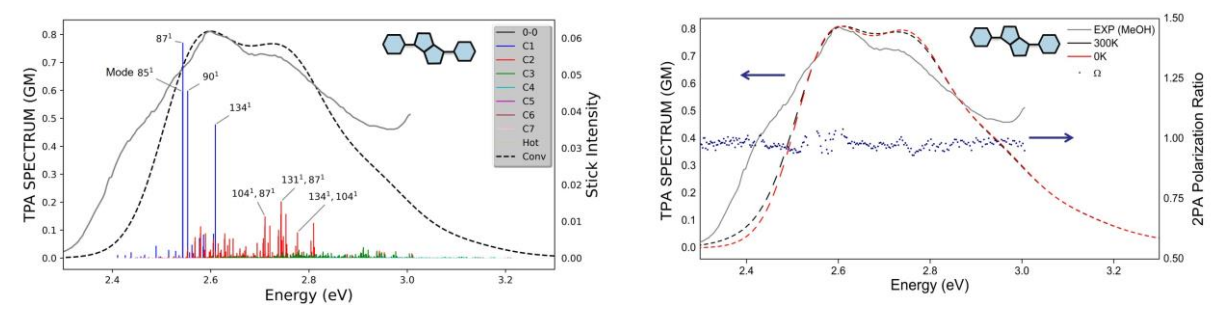


Figure 4. Calculated vibronic spectra of PDP in gas phase using TI model (FCHT, Bu-subset, 300K), left panel and TD model (FCHT, Bu-subset), right panel. Reference spectrum measured in MeOH.

The calculated 2PA profiles were shifted (by approximately 0.05~eV in the gas phase) and scaled to achieve the best alignment with the measured counterparts. The Gaussian HWHM broadening factor close to 0.075~eV was applied for both TI and TD simulations. We observed no difference in vibronic shape and composition of PDP obtained for the subset of normal modes of B_u symmetry as compared to calculations over entire vibrational space. Therefore, only the former results are shown and analyzed below.

We start our discussion focusing on HPDP, relying on AH model and FC expansion for calculation of 2PA vibronic profile in methanol (Fig. 3, left) where we observe an excellent match with the measured counterpart, just as expected for the structure with relaxed selection rules. Although HT treatment was not applied for this structure, the successful FC-based description of 2PA vibronic properties points to marked differences with e.g. Rhodamine B and the structures alike.

Next, we turn our attention to inversion-symmetric PDP, where the gas-phase results (Fig. 4) exhibit a remarkable agreement with the experimental data in vibronic shape near the 954 nm maximum as well as for the higher lying portion of the spectrum. As one may expect, there is no substantial difference between 2PA vibronic profiles from TD and TI calculations and the temperature dependence shown for TD model is negligible. Even if TI calculations require some extra CPU time to complete, especially for elevated simulation temperatures, they are also more insightful as compared to the fast TD approach. At the maximum, the spectrum is primarily shaped by a select few vibrational modes of B_u symmetry (specifically modes that we designate as 85, 87, 90, and 134, each excited with one quantum of vibrational energy). Meanwhile, the pairwise combinations of these modes with others of either B_u or A_g symmetry contribute to the higher-energy vibronic features. The displacement patterns of selected normal modes of B_u and A_g symmetry being involved in vibronic enhancement are shown in Fig. 5.

Figure 5. Displacement patterns for selected PDP B_u symmetry modes (modes 85 and 90) and A_g symmetry modes (modes 104 and 131), respectively

This description aligns well with experimental observations of the two-photon polarization ratio shown in Fig. 4 (right), which remains constant ($\Omega=0.95$) across the entire vibronic region, excluding A_u vibrations that increase this ratio to $\Omega=3/2.^{34}$ The constant nature of this polarization ratio implies that higher-lying vibronic bands retain the same total symmetry as lower bands, and may be described as a few select B_u modes augmented by vibronic progression of either A_g or other B_u modes, as anticipated by computational methods. Surprisingly, this ratio extends to the red-edge, indicating that this B_u -broken symmetry is maintained even at low-energies, perhaps indicating phonon enhancement of such vibrations.

In the low-energy 2PA region, we focus our modelling to the experimentally observed red shoulder, the location of which aligns with several modes of low coupling intensity (i.e., modes 6, 12, 21, and 49). However, these modes only marginally increase the 2PA cross-sections, falling well below experimental observations. Although the computational VG model falls short in explaining this low-energy shoulder, we speculate that besides proposed phonon interactions, the alternative AH approach could provide somewhat better vibronic description for this particular spectral range, which may potentially also contribute to enhancement of low-energy coupling terms.

The calculated 2PA vibronic spectrum of PDP in methanol is presented in Fig. 3 (right). The closer inspection and comparison with respective gas-phase description (Fig. 4, left) reveals relative enhancement of selected mode couplings in methanol, especially for the higher-energy spectral range associated with variety of prominent combination modes. The observed enhancement increases calculated intensity of the higher vibronic band in methanol, leading to higher deviation from the measured spectrum relative to gas-phase prediction. This could arise from lowering of the structural symmetry of PDP from C_{2h} in the gas phase to C₂ in methanol, manifested by the presence of non-zero values in corresponding relaxed 2PA tensor, whereas 2PA tensor is perfectly vanished in the gas phase.

4. CONCLUSIONS

We successfully applied reduced dimensionality scheme to tackle the otherwise prohibitive task of numerical differentiation of 2PA transition tensor by defining consistent subset of pre-selected normal modes based on symmetry arguments. This approach involves estimating normal modes symmetries and creating displacements along the modes capable of coupling with electronic transition of interest for subsequent calculation of derivatives of 2PA tensors. This enables computation of the relevant HT expansion terms and establishing vibronic profiles for inversion-symmetric chromophores of reasonable size. Our computational results above 2.5 eV are in excellent agreement with recently reported experimental 2PA spectrum of PDP.

These findings represent an important step in the modeling of two-photon forbidden transitions, offering an efficient means of predicting vibronic coupling based on allowable symmetry terms and thereby reducing the computational cost of modeling 2PA non-Condon effects. The results obtained indicate that, compared to calculations over a full vibrational space, a subset of vibrational modes of B_u symmetry provides all essential derivatives of the 2PA tensor for the successful description of non-Condon 2PA effects in the studied symmetric diketopyrrolopyrrole, with the exception of the red-edge shoulder. This insight could potentially define a new cost-effective approach for modeling vibronic 2PA features across a variety of symmetric chromophores.

ACKNOWLEDGEMENTS

This work was supported by the Ministry of Education and Research, Republic of Estonia (grants PRG661, PSG317). A.R. acknowledges support from NSF Award 210362. Quantum chemical calculations were carried out at the High-Performance Computing Center of the University of Tartu.

REFERENCES

- [1] Makarov, N. S., Drobizhev, M. and Rebane, A., "Two-photon absorption standards in the 550–1600 nm excitation wavelength range," Opt. Express 16(6), 4029–4047 (2008). https://doi.org/10.1364/OE.16.004029
- [2] Drobizhev, M., Makarov, N. S., Tillo, S. E., Hughes, T. E. and Rebane, A., "Describing Two-Photon Absorptivity of Fluorescent Proteins with a New Vibronic Coupling Mechanism," J. Phys. Chem. B 116(5), 1736–1744 (2012). https://doi.org/10.1021/jp211020k
- [3] Kamarchik, E. and Krylov, A. I., "Non-Condon Effects in the One- and Two-Photon Absorption Spectra of the Green Fluorescent Protein," J. Phys. Chem. Lett. 2(5), 488–492 (2011). https://doi.org/10.1021/jz101616g
- [4] Fasheng Chen, X. Z. and Liang, W., "One- and two-photon absorption spectra of the yellow fluorescent protein citrine: effects of intramolecular electron-vibrational coupling and intermolecular interactions," Mol. Phys. 116(7–8), 885–897 (2018). https://doi.org/10.1080/00268976.2018.1426130
- [5] Smith, W. L., "The Franck-Condon principle, two-photon spectroscopy and the Ã1B2u-Ã1A1g system of benzene," J. Mol. Spectrosc. 219(2), 227-237 (2003). https://doi.org/10.1016/S0022-2852(03)00051-1
- [6] de Wergifosse, M., Houk, A. L., Krylov, A. I. and Elles, C. G., "Two-photon absorption spectroscopy of trans-stilbene, cis-stilbene, and phenanthrene: Theory and experiment," J. Chem. Phys. 146(14) (2017). https://doi.org/10.1063/1.4979651
- [7] Ma, H., Zhao, Y. and Liang, W., "Assessment of mode-mixing and Herzberg-Teller effects on two-photon absorption and resonance hyper-Raman spectra from a time-dependent approach," J. Chem. Phys. 140(9) (2014). https://doi.org/10.1063/1.4867273
- [8] Zaleśny, R., Murugan, N. A., Tian, G., Medved', M. and Ågren, H., "First-Principles Simulations of One- and Two-Photon Absorption Band Shapes of the Bis(BF2) Core Complex," J. Phys. Chem. B 120(9), 2323–2332 (2016). https://doi.org/10.1021/acs.jpcb.5b09726
- [9] Bednarska, J., Zaleśny, R., Tian, G., Murugan, N. A., Ågren, H. and Bartkowiak, W., "Nonempirical Simulations of Inhomogeneous Broadening of Electronic Transitions in Solution: Predicting Band Shapes in One- and Two-Photon Absorption Spectra of Chalcones," Molecules 22(10), 1643 (2017). https://doi.org/10.3390/molecules22101643
- [10] Liang, W., Ma, H., Zang, H. and Ye, C., "Generalized time-dependent approaches to vibrationally resolved electronic and Raman spectra: Theory and applications," Int. J. Quantum Chem. 115(9), 550–563 (2015). https://doi.org/10.1002/qua.24824
- [11] Silverstein, D. W. and Jensen, L., "Vibronic coupling simulations for linear and nonlinear optical processes: Theory," J. Chem. Phys. 136(6) (2012). https://doi.org/10.1063/1.3684236
- [12] Cerezo, J. and Santoro, F., "FCclasses3: Vibrationally-resolved spectra simulated at the edge of the harmonic approximation," J. Comput. Chem. 44(4), 626–643 (2023). https://doi.org/10.1002/jcc.27027
- [13] Stark, C. W., Rammo, M., Trummal, A., Uudsemaa, M., Pahapill, J., Sildoja, M.-M., Tshepelevitsh, S., Leito, I., Young, D. C., Szymański, B., Vakuliuk, O., Gryko, D. T. and Rebane, A., "On-off-on Control of Molecular Inversion Symmetry via Multi-stage Protonation: Elucidating Vibronic Laporte Rule," Angew. Chem. 134(51), e202212581 (2022). https://doi.org/10.1002/ange.202212581

- [14] Mennucci, B., Cancès, E. and Tomasi, J., "Evaluation of Solvent Effects in Isotropic and Anisotropic Dielectrics and in Ionic Solutions with a Unified Integral Equation Method: Theoretical Bases, Computational Implementation, and Numerical Applications," J. Phys. Chem. B 101(49), 10506–10517 (1997). https://doi.org/10.1021/jp971959k
- [15] Cancès, E., Mennucci, B. and Tomasi, J., "A new integral equation formalism for the polarizable continuum model: Theoretical background and applications to isotropic and anisotropic dielectrics," J. Chem. Phys. 107(8), 3032–3041 (1997). https://doi.org/10.1063/1.474659
- [16] Becke, A. D., "Density-functional thermochemistry. III. The role of exact exchange," J. Chem. Phys. 98(7), 5648–5652 (1993). https://doi.org/10.1063/1.464913
- [17] Lee, C., Yang, W. and Parr, R. G., "Development of the Colle-Salvetti correlation-energy formula into a functional of the electron density," Phys. Rev. B 37(2), 785–789 (1988). https://doi.org/10.1103/PhysRevB.37.785
- [18] Frisch, M. J., Pople, J. A. and Binkley, J. S., "Self-consistent molecular orbital methods 25. Supplementary functions for Gaussian basis sets," J. Chem. Phys. 80(7), 3265–3269 (1984). https://doi.org/10.1063/1.447079
- [19] Frisch, M. J., Trucks, G. W., Schlegel, H. B., Scuseria, G. E., Robb, M. A., Cheeseman, J. R., Scalmani, G., Barone, V., Mennucci, B., Petersson, G. A., Nakatsuji, H., Caricato, M., Li, X., Hratchian, H. P., Izmaylov, A. F., Bloino, J., Zheng, G., Sonnenberg, J. L., Hada, M., et al., Gaussian 16 Revision C.01, Gaussian Inc. Wallingford CT (2016).
- [20] Runge, E. and Gross, E. K. U., "Density-Functional Theory for Time-Dependent Systems," Phys. Rev. Lett. 52(12), 997–1000 (1984). https://doi.org/10.1103/PhysRevLett.52.997
- [21] Yanai, T., Tew, D. P. and Handy, N. C., "A new hybrid exchange–correlation functional using the Coulomb-attenuating method (CAM-B3LYP)," Chem. Phys. Lett. 393(1–3), 51–57 (2004). https://doi.org/10.1016/j.cplett.2004.06.011
- [22] Uudsemaa, M., Trummal, A., Reguardati, S. de, Callis, P. R. and Rebane, A., "TD-DFT calculations of one- and two-photon absorption in Coumarin C153 and Prodan: attuning theory to experiment," Phys. Chem. Chem. Phys. 19(42), 28824–28833 (2017). https://doi.org/10.1039/C7CP04735E
- [23] Aidas, K., Angeli, C., Bak, K. L., Bakken, V., Bast, R., Boman, L., Christiansen, O., Cimiraglia, R., Coriani, S., Dahle, P., Dalskov, E. K., Ekström, U., Enevoldsen, T., Eriksen, J. J., Ettenhuber, P., Fernández, B., Ferrighi, L., Fliegl, H., Frediani, L., et al., "The Dalton quantum chemistry program system," WIREs Comput Mol Sci 4(3), 269–284 (2014). https://doi.org/10.1002/wcms.1172
- [24] Dalton, a molecular electronic structure program, Release Dalton V2018.2 (2019)., (see http://daltonprogram.org).
- [25] Lin, N., Santoro, F., Rizzo, A., Luo, Y., Zhao, X. and Barone, V., "Theory for Vibrationally Resolved Two-Photon Circular Dichroism Spectra. Application to (R)-(+)-3-Methylcyclopentanone," J. Phys. Chem. A 113(16), 4198–4207 (2009). https://doi.org/10.1021/jp8105925
- [26] Santoro, F., Improta, R., Lami, A., Bloino, J. and Barone, V., "Effective method to compute Franck-Condon integrals for optical spectra of large molecules in solution," J. Chem. Phys. 126(8) (2007). https://doi.org/10.1063/1.2437197
- [27] Santoro, F., Lami, A., Improta, R. and Barone, V., "Effective method to compute vibrationally resolved optical spectra of large molecules at finite temperature in the gas phase and in solution," J. Chem. Phys. 126(18) (2007). https://doi.org/10.1063/1.2721539
- [28] Santoro, F., Lami, A., Improta, R., Bloino, J. and Barone, V., "Effective method for the computation of optical spectra of large molecules at finite temperature including the Duschinsky and Herzberg–Teller effect: The Qx band of porphyrin as a case study," J. Chem. Phys. 128(22) (2008). https://doi.org/10.1063/1.2929846
- [29] Santoro, F. and Barone, V., "Computational approach to the study of the lineshape of absorption and electronic circular dichroism spectra," Int. J. Quantum Chem. 110(2), 476–486 (2010). https://doi.org/10.1002/qua.22197
- [30] Lami, A. and Santoro, F., "Time-Dependent Approaches to Calculation of Steady-State Vibronic Spectra: From Fully Quantum to Classical Approaches," [Computational Strategies for Spectroscopy], V. Barone, Ed., Wiley, 475–516 (2011). https://doi.org/10.1002/9781118008720.ch10
- [31] Ferrer, F. J. A., Cerezo, J., Soto, J., Improta, R. and Santoro, F., "First-principle computation of absorption and fluorescence spectra in solution accounting for vibronic structure, temperature effects and solvent inhomogenous broadening," Comput. Theor. Chem. 1040–1041, 328–337 (2014). https://doi.org/10.1016/j.comptc.2014.03.003
- [32] Ferrer, F. J. A. and Santoro, F., "Comparison of vertical and adiabatic harmonic approaches for the calculation of the vibrational structure of electronic spectra," Phys. Chem. Chem. Phys. 14(39), 13549–13563 (2012). https://doi.org/10.1039/C2CP41169E
- [33]Bain, A. J., "Multiphoton Processes," [Photonics], 279–320 (2015). https://doi.org/10.1002/9781119009719.ch9
- [34] Callis, P. R., "The Theory of Two-Photon-Induced Fluorescence Anisotropy," [Topics in Fluorescence Spectroscopy: Volume 5: Nonlinear and Two-Photon-Induced Fluorescence], J. R. Lakowicz, Ed., Springer US, Boston, MA, 1–42 (2002). https://doi.org/10.1007/0-306-47070-5_1